J. Dairy Sci. 107:10373–10382
https://doi.org/10.3168/jds.2024-25439
© 2024, The Authors. Published by Elsevier Inc. on behalf of the American Dairy Science Association®.
This is an open access article under the CC BY license (https://creativecommons.org/licenses/by/4.0/).

The influence of surface properties on the cooperative behavior of powdered milks

Lubomir Lapčík,[1,2]* Barbora Lapčíková,[1,2] Martin Vašina,[2,3] Eva Otyepková,[1] Alexandra Rancová,[1] Richardos Nikolaos Salek,[2] and Libor Kvítek[1]
[1]Faculty of Science, Palacky University Olomouc, 771 46, Olomouc, Czechia
[2]Faculty of Technology, Tomas Bata University in Zlín, 760 01, Zlín, Czechia
[3]Faculty of Mechanical Engineering, VSB-Technical University of Ostrava, 708 33 Ostrava, Czechia

ABSTRACT

This study comprehensively analyzes various powdered milk samples to elucidate their structural, surface, and mechanical properties. Through detailed examination, diverse characteristics among the samples were observed, shedding light on their behavior under different conditions. Notably, findings reveal intriguing insights into surface energy profiles, Harkins spreading coefficient, powder rheological properties, and sound absorption efficiency of the powdered milk samples. The intricate relationship between surface properties and bulk characteristics influenced the cooperative behavior of freely poured and consolidated milk powder beds, resulting in varying flowability from free-flowing to cohesive. Surface energy played a significant role in cohesiveness and dispersibility, with milk fat acting as a key mediator leading to changes in bulk dynamic-mechanical stiffness. These findings hold practical implications for formulating innovative aerosol-based dairy and cosmetic products, thereby enhancing everyday experiences.
Key words: powder milk, yield locus, DSC, vibro-acoustic testing, SEA

INTRODUCTION

The intricate compositional nuances of mammalian milk, varying across species, present a rich landscape of nutritional diversity (Claeys et al., 2014). Bovine milk, recognized for its moderate fat content, showcases substantial CN and whey proteins, accompanied by heightened levels of calcium, phosphorus, and vitamins A and D (McSweeney and O'Mahony, 2015). In contrast, ovine milk distinguishes itself through heightened fat and superior protein concentration, coupled with increased specific minerals and vitamins (Salimei and Fantuz, 2012). Camelid milk, although typically lower in fat and protein, often reveals enrichment in iron and vitamin C (Al Nohair, 2021). Equine milk, characterized by reduced fat and protein content, maintains comparable lactose levels to bovine milk, complemented by essential minerals and vitamins. Caprine milk, marginally fattier than bovine milk, sustains a parallel protein, mineral, and vitamin profile, subject to individual variations shaped by factors such as diet, age, and health (Raynal-Ljutovac et al., 2008). Donkey milk's structural resemblance to human breast milk is a notable highlight (Altomonte et al., 2019).

A recent ground-breaking study has shed light on a fascinating dimension of mammalian biology. Exploring nursing mice, researchers unearthed that γ-linolenic acid, a fatty acid inherent in maternal milk, intricately binds to retinoid X receptors in newborn cardiomyocytes. This unprecedented discovery reveals a profound role for a mother's milk in steering the maturation of her offspring's heart (Zhou and Pu, 2023). Notably, the study unveils the indispensable nature of γ-linolenic acid in maternal milk for normal activation of mitochondrial and fatty acid oxidation genes in the neonatal heart, opening new avenues for understanding developmental processes (Paredes et al., 2023).

Additionally, γ-linolenic acid content was found to increase from 3.09 mg/g fat in fresh milk to 3.26 mg/g fat in fermented milk in both donkey and goat milks, showcasing a dynamic response to fermentation. Beyond this, the notion of aerosolizing or pulverizing milk products sparks intriguing possibilities with potential applications in diverse fields. Whether creating powdered milk products in the food industry or exploring inhalable therapeutics in the pharmaceutical realm, the specific benefits and applications of aerosolized milk products are poised to offer innovative insights, contingent upon the distinctive properties of individual milk components. This comprehensive exploration into the realms of milk composition, developmental biology, and potential applications underscores the multifaceted significance of this pivotal biological fluid (Faye and Konuspayeva,

Received July 15, 2024.
Accepted August 22, 2024.
*Corresponding author: lapcik@utb.cz

The list of standard abbreviations for JDS is available at adsa.org/jds-abbreviations-24. Nonstandard abbreviations are available in the Notes.

2012). Therefore, the objective of this study was focused on the characterization of the bulk cooperative properties of the powdered milk samples, including surface energy distributions and profiles, vibro-acoustic and powder rheology properties, scanning electron microscopy, and thermal analysis.

MATERIALS AND METHODS

For the study, commercially available samples of powdered milks from various mammalian origins were purchased from a local store. Detailed specifications of the manufacturer can be found in Table 1. The moisture content of the powdered samples was approximately 3.5 wt %. No human or animal subjects were used, so this analysis did not require approval by an Institutional Animal Care and Use Committee or Institutional Review Board.

Scanning Electron Microscopy

Scanning electron microscopy technique was employed to visualize the structure of the powdered milks under investigation. Powdered milk samples were affixed to double-sided carbon tape and positioned on a copper holder. Subsequently, all samples underwent coating with a 10-nm layer of cobalt. Individual images were captured using an electron microscope, specifically the LVEM5 model from Delong Instruments Inc. (Brno, Czech Republic), operating in scanning electron microscopy backscattered electron mode. The accelerating voltage was set to 5.2 keV. The magnification of the individual images ranged from 1,600× to 2,300× (labeled as Magnif. 1.6k–2.3k in the original snapshots).

Surface Energy Analysis (SEA)

Inverse gas chromatography (**iGC**) was carried out using a surface energy analyzer (Surface Measurement Systems Ltd., London, UK). Samples were positioned in 4-mm (internal diameter) columns, providing a total surface area of approximately 0.5 m^2. The following eluent vapors were passed through the column: nonane, octane, hexane, and heptane. All reagents were sourced from Sigma-Aldrich (St. Louis, MO) and met analytical grade standards. The injection of vapors was meticulously controlled to ensure a predetermined fractional coverage of the sample within the column. The retention time of the vapors by the particles provides insights into the surface properties of the material, including surface energy. By progressively increasing the injected vapor amount, it becomes possible to generate a surface heterogeneity plot. For theoretical background of SEA methodology see Mohammadi-Jam and Waters (2014) and Lapčík et al. (2016).

Specific Surface Area Measurements

Specific surface area measurements of the studied samples were conducted using the nitrogen Brunauer-Emmett-Teller technique on a Micromeritics TriStar 3000 surface area and porosity analyzer (Micromeritics, Ltd., Norcross, GA). The specific surface areas of the studied milk powders were approximately 0.6 m^2/g, which was

Table 1. Labeling, description, and proximate analysis results of the studied milk powder samples[1]

Sample	Sample description	DM content (g/100 g)	Fat content (g/100 g)	Protein content (mg/g)	Bulk density (g/mL)
1	Ewe milk powder (Ekokoza Ltd., Fryčovice, Czechia)	98.12 ± 0.06^{ab}	5.77 ± 0.04^{a}	267.01 ± 11.63^{a}	0.471 ± 0.005^{a}
2	Camel milk powder (As Fresh; DNS Global Foods, Ltd., Savli, Gujarat, India)	99.54 ± 0.02^{a}	25.69 ± 0.16^{b}	277.51 ± 9.12^{a}	0.413 ± 0.004^{b}
3	Donkey milk powder (Ekokoza Ltd., Fryčovice, Czechia)	98.42 ± 0.10^{a}	1.26 ± 0.17^{c}	177.90 ± 9.59^{bd}	0.740 ± 0.007^{c}
4	Mare milk powder (Ekokoza Ltd., Fryčovice, Czechia)	99.85 ± 0.01^{ac}	1.81 ± 0.77^{cd}	172.32 ± 9.13^{b}	0.495 ± 0.004^{d}
5	Goat milk powder (Hye Foods Ltd., Rajasthan, India)	98.46 ± 0.10^{a}	24.91 ± 0.30^{bc}	253.14 ± 10.33^{a}	0.292 ± 0.003^{e}
6	Goat milk powder (Goldim Ltd., Prague, Czechia)	99.12 ± 0.75^{a}	12.33 ± 0.24^{f}	173.91 ± 10.27^{bc}	0.531 ± 0.004^{f}

[a–f]Different superscript letters within a row indicate statistically significant differences ($P < 0.05$) between the values determined. The results were expressed as arithmetic mean (n = 3) ± SE.

[1]The Tukey test was applied for multiple comparisons of the mean values to assess statistical significance, that is, to evaluate whether the differences were greater than what would be expected by chance.

consistent with values available in the literature (Berlin et al., 1964; Lapčík et al., 2015).

Yield Locus Measurements

Yield locus measurements were performed using an FT4 Powder rheometer (Freeman Technology Ltd., Tewkesbury, UK). All experiments were conducted under ambient laboratory conditions, with a temperature of 25°C and a relative humidity of 43%.

Impedance Tube Sound Absorption Measurements

The sound absorption testing was conducted using the impedance tube method based on the ISO 10534–2 standard's transfer function methodology (ISO, 2023). The frequency-dependent sound absorption coefficients were experimentally measured across the frequency spectrum of 200 to 6,400 Hz. This was accomplished using a 2-microphone impedance tube (BK 4206) in conjunction with a 3-channel signal PULSE multi-analyzer (BK 3560-B-030) and a power amplifier (BK 2706), all instrumentation sourced from Brüel & Kjær (Nærum, Denmark). The assessment specifically focused on the absorption of normal incidence sound waves by loose milk powders. These powders were characterized by defined powder bed heights (h) ranging from 20 to 50 mm. All experimental procedures were carried out under standard laboratory conditions, maintaining a relative humidity of 53% and a temperature of 24°C.

The longitudinal elastic coefficient (K) of the studied powder beds is comparable to the Young's modulus of elasticity for solid materials. It is directly proportional to the speed of sound (c) of the longitudinal elastic wave and is defined by the following formula (Okudaira et al., 1993; Yanagida et al., 2002):

$$K = c^2 \rho_b = \left(4 h f_{p1}\right)^2 \rho_b, \qquad [1]$$

where ρ_b is the bulk density of the powder bed and f_{p1} is the primary absorption peak frequency.

Dynamic-Mechanical Testing

The vibration damping properties of the studied milk powders were expressed by the displacement transmissibility (T_d), which is defined as follows (Rao, 2010):

$$T_d = \frac{y_2}{y_1} = \frac{a_2}{a_1}, \qquad [2]$$

where y_1 is the displacement amplitude on the input side of the tested sample and y_2 is the displacement amplitude on the output side of the tested sample, a_1 is the acceleration amplitude on the input side of the tested sample, and a_2 is the acceleration amplitude on the output side of the tested sample. The displacement transmissibility of a spring-mass-damper system, which is described by spring (stiffness k), damper (damping coefficient c), and mass m, is given by the following equation (Lapčík et al., 2020), where ω is angular frequency and ζ is damping ratio:

$$T_d = \sqrt{\frac{k^2 + \left(c \cdot \omega\right)^2}{\left(k - m \cdot \omega^2\right)^2 + \left(c \cdot \omega\right)^2}} = \sqrt{\frac{1 + \left(2 \cdot \zeta \cdot r\right)^2}{\left(1 - r^2\right)^2 + \left(2 \cdot \zeta \cdot r\right)^2}}. \qquad [3]$$

Under the condition $dT_d/dr = 0$ in the Equation [3], it is possible to obtain the frequency ratio r_0, at which the displacement transmissibility reaches its maximum value (Carrella et al., 2012; Ab Latif and Rus, 2014):

$$r_0 = \frac{\sqrt{\sqrt{1 + 8 \cdot \zeta^2} - 1}}{2 \cdot \zeta}. \qquad [4]$$

It is evident from Equation [4] that the local extreme of the displacement transmissibility is generally shifted to lower values of the frequency ratio r with an increasing damping ratio ζ (or with decreasing material mechanical stiffness k). The local extrema, that is, the maximum value of the displacement transmissibility T_{dmax}, is found at the frequency ratio r_0 from Equation [4]. The mechanical vibration tests were performed using the forced oscillation method. The displacement transmissibility T_d was experimentally measured using the BK 4810 vibrator in conjunction with a BK 3560-B-030 signal pulse multi-analyzer and a BK 2706 power amplifier over a frequency range from 2 to 800 Hz. The acceleration amplitudes a_1 and a_2 on the input and output sides of the investigated powder milk samples were recorded by BK 4393 accelerometers (Brüel & Kjær, Nærum, Denmark). Measurements of the displacement transmissibility were conducted with an inertial mass (m) of 90 g placed on the top side of the tested samples. The tested powder specimens were positioned in a metal box with the dimensions 60 mm long × 60 mm wide × 10 mm thick. Each measurement was repeated 3 times at an ambient temperature of 24°C.

Aerosol Spray Particle Size Measurements

Measurement of aerosol particle size distribution was conducted to assess the spraying behavior of individual powdered milk samples when dispersed in ethanol. The

0.1 wt % dispersions were sprayed using a pneumatic Microlife nebulizer, specifically the NEB 10 model from Microlife (Widnau, Switzerland), and were measured using the Spraytec instrument by Malvern Panalytical (Malvern, UK). The aerosol output of the nebulizer was set to 0.55 mL/min. The Spraytec apparatus was equipped with a He–Ne gas laser with a 632.8-nm light source wavelength and a 300-mm lens for measuring particle sizes ranging from 0.1 to 900 µm.

Differential Scanning Calorimetry

The differential scanning calorimetry (**DSC**) analysis was performed on the DSC 250 Discovery instrument (TA Instruments, New Castle, DE) using the T4 heat flow regimen. Calibration of the DSC instrument was carried out using an indium standard. For the measurement of samples, an open Tzero aluminum nonhermetic pan was filled with (3.2 ± 0.1) mg, and an empty pan was used as a reference. The thermogram was obtained by scanning from 25°C to 300°C with a heating ramp of 10°C/min under a nitrogen atmosphere at a flow rate of 50 mL/min. The thermal behavior of the samples was evaluated by parameters of endothermal temperature peaks: the onset melting temperature (T_o) and the melting peak temperature (T_p). Similarly, exothermal temperature peaks related to thermal decomposition were assessed. Relevant enthalpies, namely melting fusion enthalpy (ΔH_{fus}) and exothermic enthalpy (ΔH_{ex}), were calculated as the integral area below the thermogram peaks and expressed in normalized values (J/g; Lapčíková et al., 2021). For the second measurement, a hermetically sealed aluminum pan was employed. The thermogram was measured in the temperature range from −20°C to 130°C, with a heating rate of 5°C/min. The sample weight was maintained at (4.3 ± 0.2) mg. The measurements were conducted under a nitrogen atmosphere at a flow rate of 50 mL/min. Evaluated parameters included the glass transition temperature (T_g) and the thermal capacity (Δc_p; J/g °C).

Statistical Analysis

Obtained experimental data from thermal analysis (DSC) were analyzed by one-way ANOVA with Tukey's multiple range test to characterize correlations among DSC measurements. Differences in the mean values among statistical groups were tested at a significance level of $P \leq 0.05$. Sigma Plot ver. 12.5 (Systat Software, San Jose, CA) was used for data analysis.

RESULTS

As depicted in Figure 1, the powdered milk samples under investigation, as specified in Table 1, were approximately 25 µm wide in diameter, exhibited a spherical shape. A compact porous surface structure was observed in all samples, except for Sample 3, which consisted of individual particle clusters. The studied powder samples originated from different mammals and had a dry matter content of approximately 99 g/100 g. The fat content varied from 1.26 to 25.69 g/100 g. The highest fat content was detected in Samples 2 (camel milk powder) and 5 (goat milk powder from India), each at approximately 25 g/100 g. Sample 6 (goat milk powder manufactured in Czechia) had a fat content of ~12 g/100 g. Sample 1 (ewe milk powder) had a fat content of ~6 g/100 g, and Samples 3 and 4 (donkey and mare milk powders) ranged from about 1.3 to 1.8 g/100 g. The observed protein content ranged from 170 to 280 mg/g.

Surface energy profiles obtained by SEA of the studied powders are shown in Figure 2. The obtained data for total, polar, and dispersive components indicated extremely narrow dependencies on fractional surface coverage, ranging from 45 (Sample 3) to 55 mJ/m^2 (Sample 5). Minor deviation from the above-mentioned linearity of the observed surface energy profiles was found for Sample 3 (donkey milk powder), where approximately 5% of the surface was covered with 6 mJ/m^2 higher energy polar sites.

Results of the specific acid–base free energy distributions for selected polar probes (dichloromethane [**diClM**], acetone [**Ac**], and ethyl acetate [**EtAc**]) of Sample 3 are shown in Figure 3. A relatively wide range of free energies was found, ranging from 7 to 9 kJ/mol for the Ac probe and from 8.5 to 10.6 kJ/mol for the diClM probe. A narrow specific acid–base free energy distribution, ranging from 7.8 to 9 kJ/mol, was observed for the EtAc probe. However, the specific free energy distributions of the remaining samples were not possible to detect due to the high surface energy similarity of the studied powdered milk samples' surfaces, thus they did not exhibit typical distribution patterns.

The results of the calculated difference between the thermodynamic work of adhesion and the work of cohesion of water on the studied milk powders, known as the Harkins spreading coefficient (Harkins and Feldman, 1922), are shown in Figure 4. The results indicated an increasing polarity in Samples 3, 4, and 6. This polarity enhanced the spreading of water compared with Samples 1 and 5, which exhibited a more cohesive character, as indicated by the negative value of the difference between the work of adhesion and the work of cohesion.

The results of the powder rheological measurements are depicted in Figure 5 and Table 2. Sample 2 exhibited the highest cohesion of 2.43 kPa, followed by Sample 4 with 2.12 kPa, and Sample 5 with 1.9 kPa. Conversely, Sample 3 showed the lowest cohesion of 0.25 kPa, indicating the presence of the lowest total surface energy

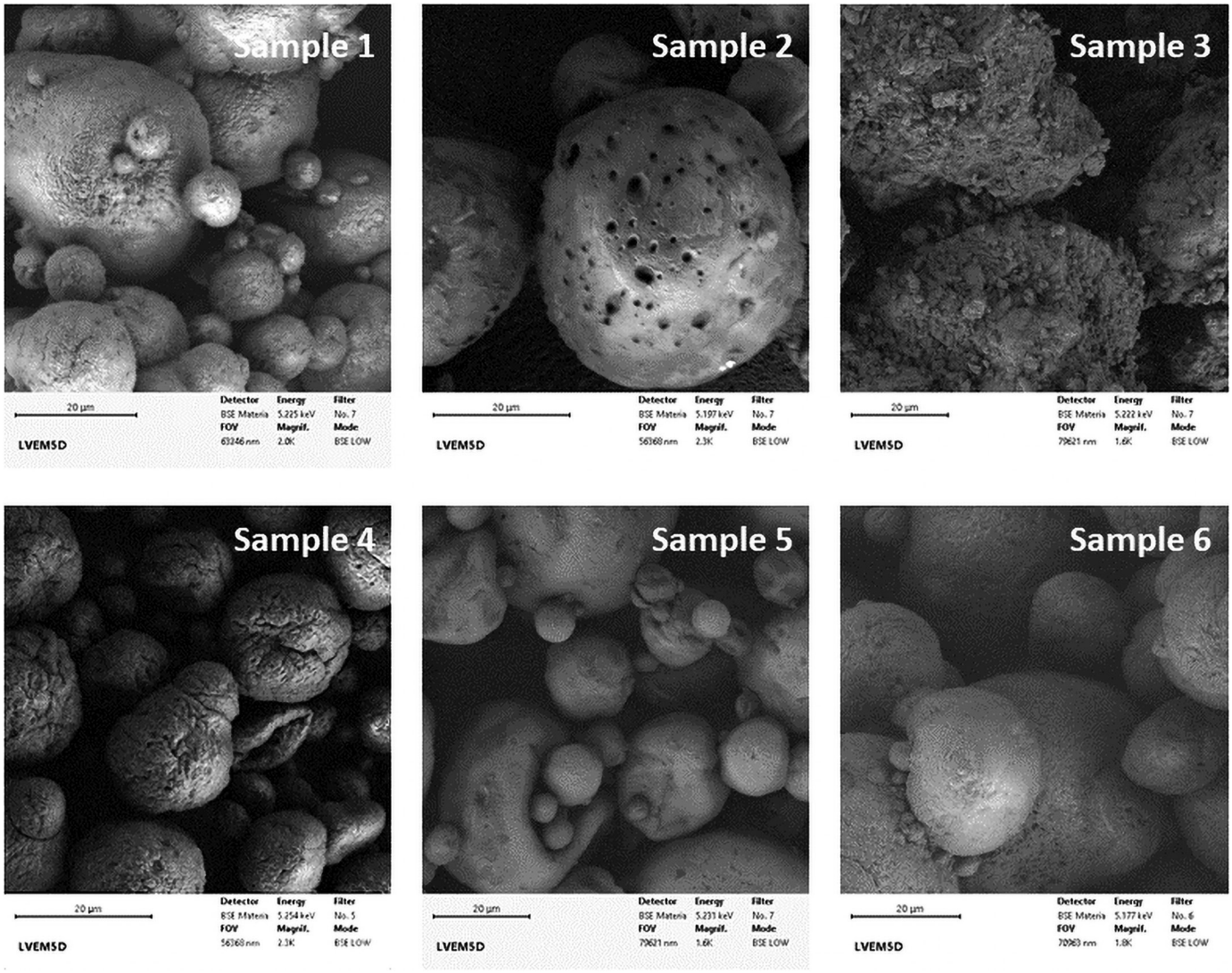

Figure 1. Scanning electron microscope images of the studied powder milk samples.

of 45 mJ/m^2 at the solid/gas interface, as confirmed by iGC SEA measurements (Figure 2). Additionally, Sample 3 displayed the highest flow function value of 16.74, surpassing the typical threshold of 10 for free-flowing powders. The frequency dependencies of the sound absorption coefficient of the studied samples are shown in Figure 6. Sample 3 exhibited the lowest sound absorption due to its compact structure, as evidenced by its highest bulk density of 0.74 g/mL (Table 1) compared with all other studied samples. In contrast, Sample 5, with the lowest bulk density of 0.292 g/mL, exhibited the highest sound absorption performance, indicating the occurrence of a highly porous powder bed structure due to the high cohesivity of individual powder particulates (cohesion of 1.9 kPa).

Figure 7A displays the data of noise reduction coefficient versus powder bed height dependencies for all samples under study. The observed experimental points were modeled as second-order polynomial functions. However, in the case of the studied powder milk samples, this behavior was associated with the increasing loose powder bed height for the majority of studied samples, except for Samples 1 and 3. The powder bed height dependencies of the longitudinal elastic coefficients (K) are shown in Figure 7B. The highest stiffness of the studied milk's freely poured powder beds was obtained for Sample 4 (K = 8 MPa), followed by Samples 2 and 5 (K = 6 MPa) for bed heights ranging from 20 to 40 mm. The results of the dynamic-mechanical testing of the studied powders are presented in Figure 8. Sample 6 dis-

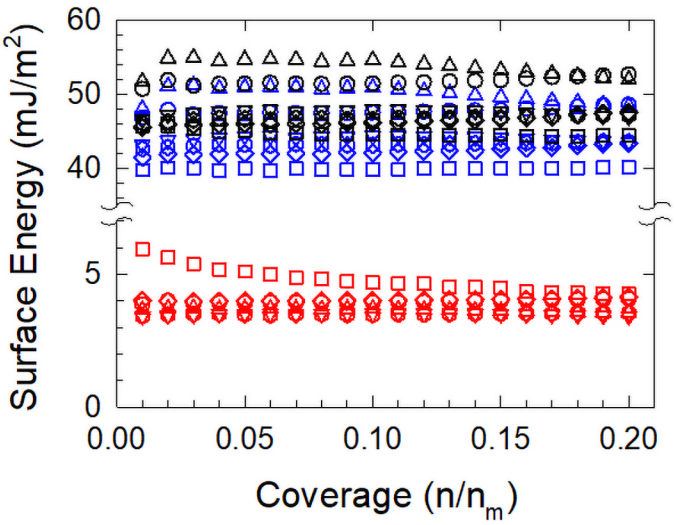

Figure 2. Surface energy profiles of the studied powdered milk samples: circle = Sample 1, inverted triangle = Sample 2, square = Sample 3, diamond = Sample 4, triangle = Sample 5, hexagon = Sample 6. Color codes: red = polar part of surface energy, blue = dispersive part of surface energy, black = total surface energy.

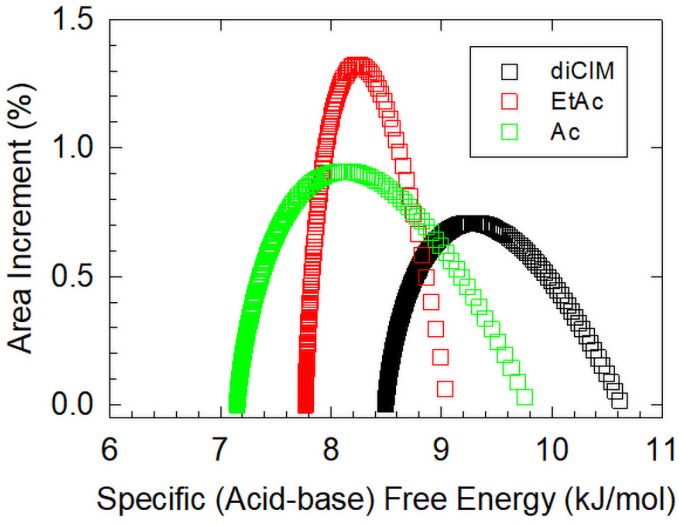

Figure 3. Specific acid–base free energy distributions of Sample 3 as observed for selected wetting probes color-coded as follows: black = dichloromethane (diClM), red = ethyl acetate (EtAc), green = acetone (Ac).

played the highest stiffness, attributed to its high packing density and material flowability.

As shown in Table 3, Sample 2 exhibited the lowest T_g at 26.82°C. Conversely, for the other samples under investigation, their T_g values were notably higher, exceeding 43°C, indicating a predominantly amorphous phase conformation under laboratory conditions. The aerosol particle size distributions are shown in Figure 9 and Table 4. Samples 2 and 5 were not evaluated due to their high tendency for agglomeration in ethanol. Results indicated the bimodal character of the particle size distribution functions of the dispersed powder milk phase in aerosol ethanol dispersive phase.

DISCUSSION

The results of the powdered milk samples show significant differences in their composition and physical properties, which are influenced by the type of milk and the processing methods used. The variation in fat content

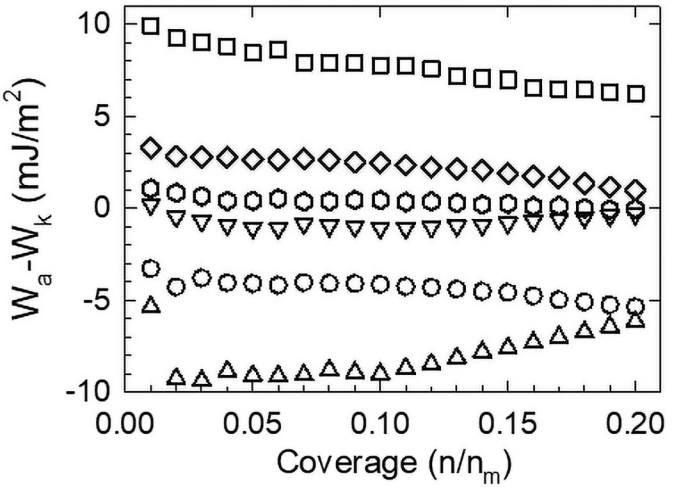

Figure 4. The difference between the work of adhesion of water on the studied milk powders and the work of cohesion of the studied milk powders presented as a function of coverage at 25°C: circle = Sample 1, inverted triangle = Sample 2, square = Sample 3, diamond = Sample 4, triangle = Sample 5, hexagon = Sample 6. W_a-W_k = work of adhesion minus work of cohesion.

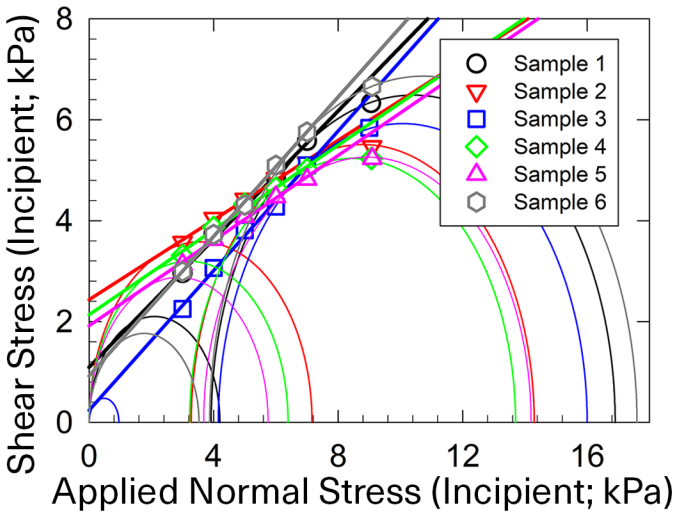

Figure 5. Powder rheology yield locus and Mohr's circles of the studied milk powders consolidated at 9 kPa preshear normal stress (measured at 25°C, 43% relative humidity).

Table 2. Results of rheological measurements for the milk powders studied using the shear cell[1]

Sample	Cohesion (kPa)	UYS (kPa)	MPS (kPa)	FF (–)	AIF (°)	MCS (kPa)
1	1.17	4.20	16.86	4.01	31.80	3.92
2	2.43	7.16	14.25	1.99	21.54	3.28
3	0.25	0.96	16.02	16.74	34.60	4.15
4	2.12	6.39	13.75	2.15	22.97	3.23
5	1.90	5.75	14.16	2.46	22.99	3.68
6	0.93	3.53	17.58	4.98	34.62	3.87

[1]Samples were consolidated at 9 kPa preshear normal stress and temperature of 25°C. The relative humidity of the ambient atmosphere was maintained at 43%. UYS = unconfined yield strength, MPS = major principal stress, FF = flow function, AIF = angle of internal friction, MCS = minor consolidation stress.

among the samples, with camel and Indian goat milk powders exhibiting the highest fat content, aligns with previous studies that have highlighted the richness of fat in these types of milk. The low-fat content in donkey and mare milk powders is consistent with their known composition, which is often lower in fat compared with another mammals' milk.

The surface energy profiles and the specific acid–base free energy distributions further emphasize the differences in the physical properties of the milk powders. The unique surface energy characteristics of Sample 3, particularly its higher energy polar sites, suggest a distinct interaction with polar probes, which may influence its behavior in various applications.

The Harkins spreading coefficient results indicate that Samples 3, 4, and 6 exhibit higher polarity, enhancing water spreading. This finding is particularly relevant for applications where moisture interaction is critical, such as in food products or pharmaceuticals.

The rheological measurements highlight the significant effect of fat content on powder cohesion. The high cohesion observed in Sample 2 correlates with its high fat content, which is known to increase interparticle interactions and, consequently, the cohesiveness of the powder (Sert et al., 2022). In contrast, the low cohesion and high flow function value of Sample 3 suggest that it would behave as a free-flowing powder, which is desirable in processes that require easy handling and transport of the powder.

The sound absorption measurements reveal 2 primary mechanisms of sound absorption in the milk powders: air friction and mechanical vibration. The high sound absorption observed in Sample 5, despite its low bulk density, can be attributed to its porous structure, which enhances the absorption of sound energy.

The dynamic-mechanical testing results further support the observations of the rheological properties, with Sample 6 exhibiting the highest stiffness due to its high

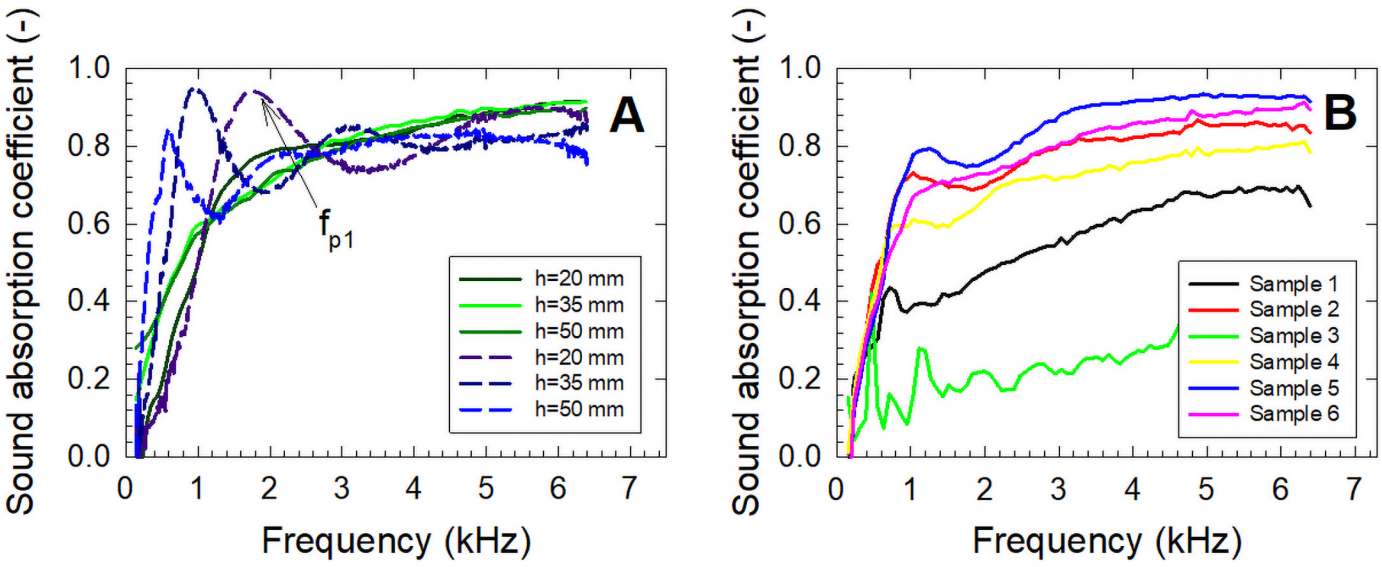

Figure 6. Frequency dependencies of the sound absorption coefficient for the studied milk powders. (A) Data for different loose powder beds (heights [h] given in the insert legend) for Samples 5 and 6. Solid line = Sample 6, dashed line = Sample 5. f_{p1} = primary absorption peak frequency. (B) Data from all samples at a powder bed height of 30 mm.

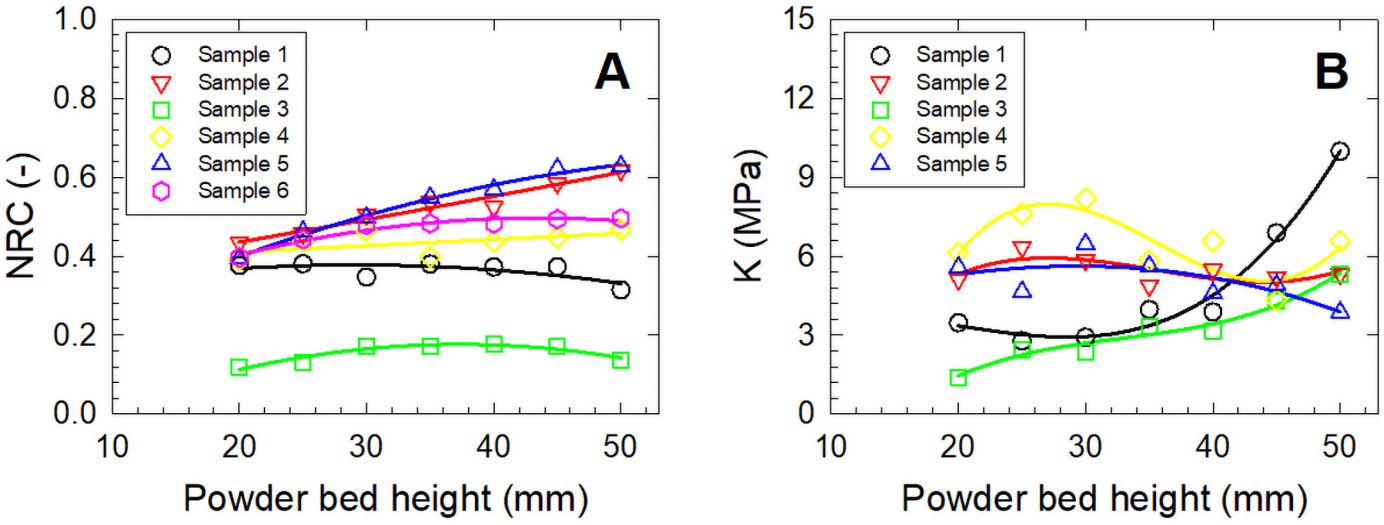

Figure 7. Results of the acoustic impedance tube measurements of studied powder milk samples. (A) Noise reduction coefficient (NRC) of the loose powder bed versus powder bed height dependencies. (B) Longitudinal elastic coefficient (K) of the loose powder bed versus powder bed height dependencies (measured at 24°C, 62% relative humidity).

packing density and material flowability. This characteristic makes it suitable for applications where mechanical stability is essential.

The thermal analysis of the samples, particularly the glass transition temperature (T_g), provides insights into the thermal stability of the powders. The lower T_g observed in Sample 2 suggests that it may be more prone to structural changes at lower temperatures, which could affect its storage and handling properties.

The aerosol particle size distribution results indicate a bimodal distribution in the samples, with variations in particle size potentially affecting their behavior in aerosolized applications. The inability to evaluate Samples 2 and 5 due to agglomeration highlights the challenges in processing powders with high fat content, which tend to clump together in dispersive mediums such as ethanol.

Table 3. Results of the thermal analysis of the studied milk powders[1]

Sample	T_g (°C)	c_P (J·g^{-1}·°C^{-1})
1	43.33 ± 1.24^{a}	0.0125 ± 0.0011^{ade}
2	26.82 ± 0.27^{b}	0.2610 ± 0.0099^{b}
3	52.04 ± 2.51^{c}	0.1135 ± 0.0315^{af}
4	59.85 ± 0.61^{d}	0.5115 ± 0.0272^{c}
5	49.47 ± 1.30^{ac}	0.0160 ± 0.0424^{d}
6	68.20 ± 0.09^{e}	0.1755 ± 0.0018^{bef}

$^{a–f}$Different superscript letters within a column indicate statistically significant differences between the values determined ($P < 0.05$). The results were expressed as arithmetic mean ± SD.

[1]T_g = glass transition temperature, c_P = specific isobaric heat capacity. Differences in the mean values among the statistical groups were tested at a significance level of $P < 0.05$. The Tukey test was applied for multiple comparisons of the mean values to assess statistical significance, that is, to evaluate whether the differences were greater than what would be expected by chance.

Overall, the results demonstrate the complex interplay between the composition and physical properties of powdered milks, with implications for their use in various industrial and consumer applications. The differences observed in surface energy, rheology, sound absorption, and thermal properties underscore the importance of selecting the appropriate type of milk powder for specific applications, depending on the desired characteristics and performance criteria.

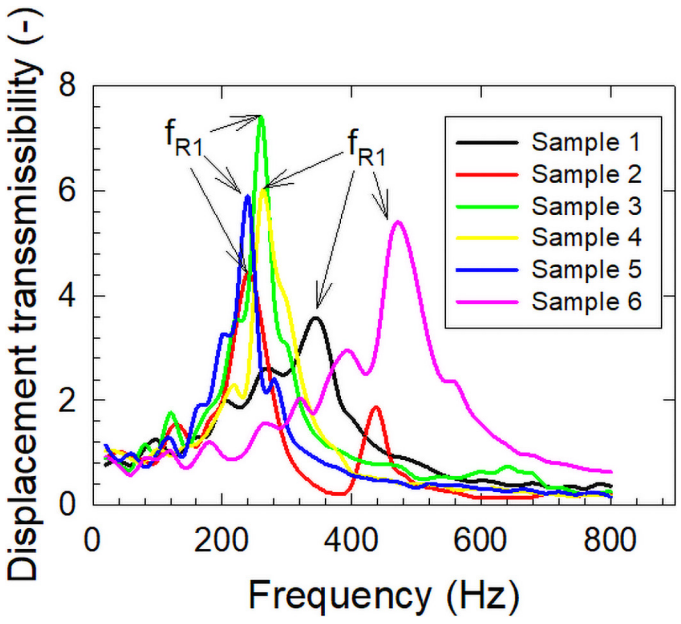

Figure 8. Frequency dependencies of the displacement transmissibility for the studied powder milk samples with applied inertial mass of 90 g (measured at 24°C, 62% relative humidity). f_{R1} = first resonance frequency.

Table 4. Results of the nebulizer particle size distribution measurements of the studied samples[1]

Sample	$d_V(10)$ (μm)	$d_V(50)$ (μm)	$d_V(90)$ (μm)	$d_{3,2}$ (μm)	$d_{4,3}$ (μm)
1	5.327	12.45	30.48	10.38	5.327
2	N/A	N/A	N/A	N/A	N/A
3	5.967	13.71	30.5	11.32	5.967
4	5.586	13.87	37.62	11.19	5.586
5	N/A	N/A	N/A	N/A	N/A
6	5.304	11.96	29.75	10.15	5.304

[1]$d_V(10)$ is the volume average diameter at which 10% of the sample's particles are finer. $d_V(50)$ is the volume average particle median. $d_V(90)$ is the volume average particle diameter, at which 90% of the sample's particles are finer. $d_{3,2}$ is the Sauter particle mean diameter. $d_{4,3}$ is the De Brouckere mean diameter, or volume-weighted particle mean diameter; N/A = not available.

CONCLUSIONS

In this study, we investigated the intricate relationship between surface properties and bulk characteristics of various milk powders. These interactions influenced the cooperative behavior of freely poured and consolidated milk powder beds, resulting in varying flowability ranging from free-flowing to cohesive. The highest flowability was found for Sample 3, which contained the lowest fat content. In contrast Sample 2, with the highest fat content, exhibited the most cohesive powder flow behavior. This indicated the enhancing role of the milk fat on powder bed structural organization. Notably, surface energy played a significant role in cohesiveness and dispersibility, with milk fat acting as a key mediator leading to changes in bulk dynamic-mechanical stiffness. These findings hold practical implications for formulating innovative aerosol-based dairy and cosmetic products, thereby enhancing our everyday experiences.

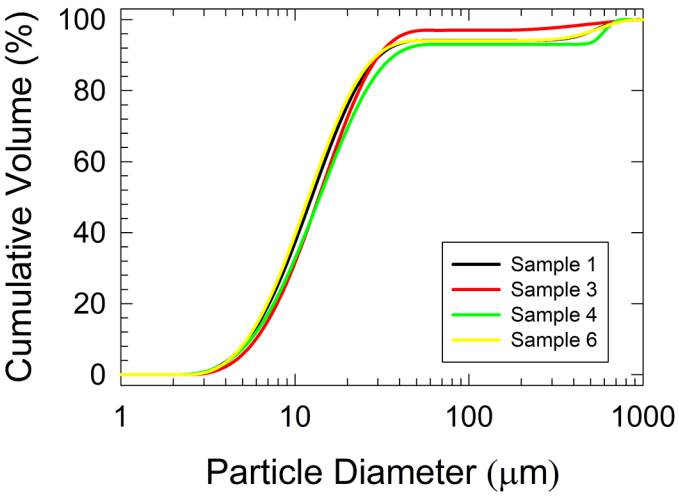

Figure 9. The nebulizer's particle size distribution of the dispersed powdered milk samples as obtained using Malvern Panalytical's (Malvern, UK) Spraytec instrument. Samples 2 and 5 were not evaluated due to their high tendency for agglomeration in ethanol. Results indicated the bimodal character of the particle size distribution functions of the dispersed powder milk phase in the aerosol ethanol dispersive phase.

NOTES

This research was funded by Tomas Bata University in Zlín, Czechia (project no. IGA/FT/2024/005) and from Palacky University Olomouc (Olomouc, Czechia; project no. IGA_PrF_2024_020). Data will be made available on request. Author contributions are as follows: L.L., conceptualization, methodology, software, validation, formal analysis, investigation, resources, data curation, writing (original draft, review and editing), visualization, and supervision; B.L., methodology, validation, investigation, data curation, writing (review and editing); M.V., methodology, validation, formal analysis, investigation, data curation, and writing (original draft, review and editing); E.O., methodology; A.R., methodology; R.N.S., software, resources, and project administration; and L.K., investigation, resources, project administration, and funding acquisition. All authors have read and agreed to the published version of the manuscript. No human or animal subjects were used, so this analysis did not require approval by an Institutional Animal Care and Use Committee or Institutional Review Board. The authors have not stated any conflicts of interest.

Nonstandard abbreviations used: Ac = acetone; AIF = angle of internal friction; diClM = dichloromethane; DSC = differential scanning calorimetry; EtAc = ethyl acetate; FF = flow function; h = height; iGC = inverse GC; MCS = minor consolidation stress; MPS = major principal stress; NRC = noise reduction coefficient; SEA = surface energy analysis; T_g = glass transition temperature; c_P = specific isobaric heat capacity; UYS = unconfined yield strength.

REFERENCES

Ab Latif, N., and A. Z. M. Rus. 2014. Vibration transmissibility study of high density solid waste biopolymer foam. J. Mech. Eng. Sci. 6:772–781. https://doi.org/10.15282/jmes.6.2014.5.0075.

Al Nohair, S. F. 2021. Medical benefits of camel's milk: A comprehensive review. J. Pak. Med. Assoc. 71:933–937.

Altomonte, I., F. Salari, R. Licitra, and M. Martini. 2019. Donkey and human milk: Insights into their compositional similarities. Int. Dairy J. 89:111–118. https://doi.org/10.1016/j.idairyj.2018.09.005.

Berlin, E., N. M. Howard, and M. J. Pallansch. 1964. Specific surface areas of milk powders produced by different drying methods. J. Dairy Sci. 47:132–138. https://doi.org/10.3168/jds.S0022-0302(64)88605-7.

Carrella, A., M. J. Brennan, T. P. Waters, and V. Lopes Jr.. 2012. Force and displacement transmissibility of a nonlinear isolator with high-static-low-dynamic-stiffness. Int. J. Mech. Sci. 55:22–29. https://doi.org/10.1016/j.ijmecsci.2011.11.012.

Claeys, W. L., C. Verraes, S. Cardoen, J. De Block, A. Huyghebaert, K. Raes, K. Dewettinck, and L. Herman. 2014. Consumption of raw or heated milk from different species: An evaluation of the nutritional and potential health benefits. Food Control 42:188–201. https://doi.org/10.1016/j.foodcont.2014.01.045.

Faye, B., and G. Konuspayeva. 2012. The sustainability challenge to the dairy sector—The growing importance of non-cattle milk production worldwide. Int. Dairy J. 24:50–56. https://doi.org/10.1016/j.idairyj.2011.12.011.

Harkins, W. D., and A. Feldman. 1922. Films. The spreading of liquids and the spreading coefficient. J. Am. Chem. Soc. 44:2665–2685. https://doi.org/10.1021/ja01433a001.

ISO (International Organization for Standardization). 2023. Acoustics—Determination of acoustic properties in impedance tubes. Part 2: Two-microphone technique for normal sound absorption coefficient and normal surface impedance. ISO 10534–2:2023. Accessed Oct. 8, 2024. https://www.iso.org/standard/81294.html.

Lapčík, L., B. Lapčíková, E. Otyepková, M. Otyepka, J. Vlček, F. Buňka, and R. N. Salek. 2015. Surface energy analysis (SEA) and rheology of powder milk dairy products. Food Chem. 174:25–30. https://doi.org/10.1016/j.foodchem.2014.11.017.

Lapčík, L., M. Otyepka, E. Otyepkova, B. Lapčíková, R. Gabriel, A. Gavenda, and B. Prudilova. 2016. Surface heterogeneity: Information from inverse gas chromatography and application to model pharmaceutical substances. Curr. Opin. Colloid Interface Sci. 24:64–71. https://doi.org/10.1016/j.cocis.2016.06.010.

Lapčík, L., M. Vasina, B. Lapčíková, M. Stanek, M. Ovsik, and Y. Murtaja. 2020. Study of the material engineering properties of high-density poly(ethylene)/perlite nanocomposite materials. Nanotechnol. Rev. 9:1491–1499. https://doi.org/10.1515/ntrev-2020-0113.

Lapčíková, B., L. Lapčík, T. Valenta, P. Majar, and K. Ondrousková. 2021. Effect of the rice flour particle size and variety type on water holding capacity and water diffusivity in aqueous dispersions. Lebensm. Wiss. Technol. 142:111082.

McSweeney, P. L., and J. A. O'Mahony. 2015. Advanced Dairy Chemistry: Volume 1B: Proteins: Applied Aspects. 4th ed. Springer, New York, NY.

Mohammadi-Jam, S., and K. E. Waters. 2014. Inverse gas chromatography applications: A review. Adv. Colloid Interface Sci. 212:21–44. https://doi.org/10.1016/j.cis.2014.07.002.

Okudaira, Y., Y. Kurihara, H. Ando, M. Satoh, and K. Miyanami. 1993. Sound-absorption measurements for evaluating dynamic physical-properties of a powder bed. Powder Technol. 77:39–48. https://doi.org/10.1016/0032-5910(93)85005-T.

Paredes, A., R. Justo-Méndez, D. Jiménez-Blasco, V. Núñez, I. Calero, M. Villalba-Orero, A. Alegre-Marti, T. Fischer, A. Gradillas, V. Sant'Anna, F. Were, Z. Q. Huang, P. Hernansanz-Agustín, C. Contreras, F. Martínez, E. Camafeita, J. Vázquez, J. Ruiz-Cabello, E. Area-Gómez, F. Sánchez-Cabo, E. Treuter, J. P. Bolaños, E. Estébanez-Perpiña, F. J. Rupérez, C. Barbas, J. A. Enríquez, and M. Ricote. 2023. Γ-linolenic acid in maternal milk drives cardiac metabolic maturation. Nature 618:365–373. https://doi.org/10.1038/s41586-023-06068-7.

Rao, S. S. 2010. Mechanical Vibrations. 5th ed. Prentice Hall, Upper Saddle River, NJ.

Raynal-Ljutovac, K., G. Lagriffoul, P. Paccard, I. Guillet, and Y. Chilliard. 2008. Composition of goat and sheep milk products: An update. Small Rumin. Res. 79:57–72. https://doi.org/10.1016/j.smallrumres.2008.07.009.

Salimei, E., and F. Fantuz. 2012. Equid milk for human consumption. Int. Dairy J. 24:130–142. https://doi.org/10.1016/j.idairyj.2011.11.008.

Sert, D., E. Mercan, and M. Kilinc. 2022. Powder flow behaviour, functional characteristics and microstructure of whole milk powder produced from cow and buffalo milk mixtures. Int. Dairy J. 135:105474. https://doi.org/10.1016/j.idairyj.2022.105474.

Yanagida, T., A. J. Matchett, J. M. Coulthard, B. N. Asmar, P. A. Langston, and J. K. Walters. 2002. Dynamic measurement for the stiffness of loosely packed powder beds. AIChE J. 48:2510–2517. https://doi.org/10.1002/aic.690481110.

Zhou, P., and W. T. Pu. 2023. Molecule in mothers' milk nurses pups' heart cells to maturity. Nature 618:242–243. https://doi.org/10.1038/d41586-023-01635-4.

ORCIDS

Lubomir Lapčík, https://orcid.org/0000-0002-9917-7310
Barbora Lapčíková, https://orcid.org/0000-0002-4713-0502
Martin Vašina, https://orcid.org/0000-0002-8506-098X
Richardos Nikolaos Salek, https://orcid.org/0000-0001-5129-5329